MANUSCRIPT

Title: Trophic interactions shape the spatial organization of medium-chain carboxylic acid producing granular biofilm communities

Pieter Candry[1,2], Grayson L. Chadwick[3], José Maria Caravajal-Arroyo[1], Tim Lacoere[1], Mari Karoliina-Henriikka Winkler[2], Ramon Ganigué[1,4], Victoria J. Orphan[3a], Korneel Rabaey[1,4]

[1] Center for Microbial Ecology and Technology (CMET), Ghent University, Coupure Links 653, 9000 Ghent, Belgium

[2] Civil and Environmental Engineering, University of Washington, 201 More Hall, Box 352700, Seattle, WA 98195-2700, USA

[3] Division of Geological and Planetary Sciences, California Institute of Technology, Pasadena, California 91125, USA

[4] Center for Advanced Processes and Technology for Urban Resource recovery (CAPTURE), Frieda Saeysstraat 1, 9000 Ghent, Belgium

* Correspondence to: Korneel Rabaey, Ghent University; Faculty of Bioscience Engineering; Centre for Microbial Ecology and Technology (CMET); Coupure Links 653; B-9000 Gent, Belgium; phone: +32 (0)9 264 59 76; fax: +32 (0)9 264 62 48; E-mail: Korneel.Rabaey@UGent.be; Webpage: www.cmet.UGent.be.

Abstract

Granular biofilms producing medium-chain carboxylic acids (MCCA) from carbohydrate-rich industrial feedstocks harbor highly streamlined communities converting sugars to MCCA either directly or via lactic acid as intermediate. We investigated the spatial organization and growth activity patterns of MCCA producing granular biofilms grown on an industrial side stream to test (i) whether key functional guilds (lactic acid producing *Olsenella* and MCCA producing Oscillospiraceae) stratified in the biofilm based on substrate usage, and (ii) whether spatial patterns of growth activity shaped the unique, lenticular morphology of these biofilms. First, three novel isolates (one *Olsenella* and two Oscillospiraceae species) representing over half of the granular biofilm community were obtained and used to develop FISH probes, revealing that key functional guilds were not stratified. Instead, the outer 150-500 µm of the granular biofilm consisted of a well-mixed community of *Olsenella* and Oscillospiraceae, while deeper layers were made up of other bacteria with lower activities. Second, nanoSIMS analysis of ^{15}N incorporation in biofilms grown in normal and lactic acid amended conditions suggested Oscillospiraceae switched from sugars to lactic acid as substrate. This suggests competitive-cooperative interactions may govern the spatial organization of these biofilms, and suggests that optimizing biofilm size may be a suitable process engineering strategy. Third, growth activities were similar in the polar and equatorial biofilm peripheries, leaving the mechanism behind the lenticular biofilm morphology unexplained. Physical processes (e.g., shear hydrodynamics, biofilm life cycles) may have contributed to lenticular biofilm development. Together, this study develops an ecological framework of MCCA-producing granular biofilms that informs bioprocess development.

1. Introduction

Medium-chain carboxylic acids (MCCA) are saturated monocarboxylic acids with 6 to 12 carbon chains that have been proposed as a target for bioproduction from organic-rich industrial wastes and industrial side streams. They are readily produced by fermentative open microbial communities, are more easily recovered than short-chain carboxylic acids such as acetic or lactic acid, and have potential as chemical building blocks for solvents, flavors, and fuels (1–3). Recently, granular biofilm technologies have enabled overcoming limitations of volumetric production rates that have hindered implementation of MCCA production systems (4–8). These systems can achieve higher biomass concentrations than suspended growth bioreactors without the energy expenses associated with membrane bioreactor technologies (9). While granular biofilms are a promising avenue for MCCA production technologies, key aspects of these systems' microbial ecology remain unexplored.

Granular biofilms producing MCCA from real waste streams without external electron donors have only been reported in two studies using thin stillage, a side-stream from the bioethanol industry (5,7). The biofilm community in these systems was highly enriched, with 5 operational taxonomic units (OTU) accounting for over 80% of the community (5). Conversion of sugars to MCCA in these communities is hypothesized to occur through two parallel pathways (Figure 1). In a first pathway, sugars are first converted by *Olsenella* to lactic acid (10), which can then be converted to MCCA by, for instance, relatives of Oscillospiraceae bacterium CPB6 (11). In the second pathway, sugars could potentially be converted directly to MCCA by community members closely related to the Oscillospiraceae-member *Caproiciproducens galactitolivorans* (12). These two parallel pathways may result in both competitive and cooperative interactions controlling the activities of community members. Moreover, several MCCA producing organisms have now been shown to consume lactic acid and carbohydrates, blurring the lines between these functional guilds (13,14). Understanding

the *in-situ* carbon fluxes and ecological interactions among community members is a critical challenge in MCCA producing microbiomes in order to develop rational process optimization and control strategies (15).

The MCCA producing granules were approximately 3 mm in size and displayed a lenticular - or disc-shaped - morphology with 2 long axes and 1 short axis (5). This morphology was hypothesized to be driven by substrate and product gradients, factors that could also affect – and be affected by – the spatial organization of the community (Figure 1, Figure S.1.). First, substrate and product gradients could limit growth rates deeper in the biofilm due to substrate limitation and MCCA toxicity (16,17). MCCA concentrations may be lower near the equatorial periphery (i.e., the rim of the disc) due to shorter diffusion path lengths than at the polar periphery (i.e., the flat surface of the disc). Higher growth rates at the rim of the disc-shaped biofilm could in turn drive biofilm growth along a plane, producing lenticular biofilms. Second, substrate and product gradients could stratify key functional guilds (i.e., *Olsenella* and Oscillospiraceae) in the biofilm. Community stratification shaped by substrate gradients is a common phenomenon in granular biofilms. For instance, oxygen gradients stratify aerobic granular sludge and nitritation-anammox biofilm communities (18,19), while stratification in methane-producing anaerobic digestion granules is shaped by gradients of carbon substrates (20). In MCCA producing biofilms, sugar consuming lactic acid producers may be enriched near the biofilm periphery while lactic acid consuming MCCA producers would dominate deeper in the granule due to substrate exchange and their potentially higher tolerance to toxic MCCA. Together, these hypotheses suggest that substrate and product gradients could have significant impacts on the morphology and microbial ecology of MCCA producing granular biofilms, which may have implications for the design and development of this bioproduction technology.

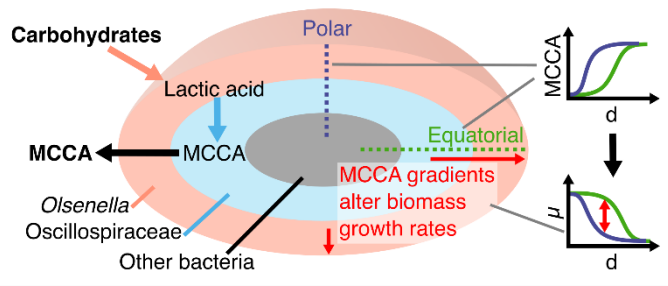

Figure 1. Initial hypothesis of carbon fluxes and mechanisms shaping lenticular biofilm morphology

In this study, we used single-cell resolved methods to investigate the spatial and microbial ecology of MCCA producing granular biofilms. We analyzed the spatial community organization with fluorescence *in situ* hybridization (FISH) to test the stratification hypothesis, while FISH coupled with the *in-situ* analysis of ^{15}N incorporation with nanoSIMS answered questions on spatial growth activity patterns and substrate usage by key functional guilds (21,22). Together, this information provides critical insights into the metabolic interactions between lactic acid and MCCA producing organisms and the spatial organization of MCCA producing granular biofilms.

2. Materials & Methods

2.1. Inoculum source

An expanded granular sludge bed (EGSB) reactor similar to that described by Carvajal-Arroyo et al. (5) was used to generate inoculum for all following experiments. Gravitationally clarified thin stillage (Supplementary Information, S.1.1.) amended with 0.95 g $NH_4Cl \cdot L^{-1}$ was used as feed for the reactor, which was operated under constant conditions; dilution rate of 2.5 d^{-1}, pH of 5.5, and a hydraulic upflow velocity of 11.25 $m \cdot h^{-1}$ maintained by recirculating the reactor broth. Granular biofilms harvested from the bioreactor reported in Carvajal-Arroyo et al. (5) were used as inoculum. Samples were taken from a sampling port in the middle of the reactor.

2.2. Isolation of key organisms

An isolation campaign was set up to isolate key functional organisms from the granular biofilms. Four different media types were used; 2 minimal media and 2 complex media based on thin stillage. Minimal media were based on literature reports for either sugar- or lactic acid-based chain elongating organisms. The minimal glucose (MG) medium was modified from the medium used to isolate *C. galactitolivorans* sp. BS-1 – a sugar alcohol-based chain elongator –, substituting D-galactitol for D-glucose (12,23). The minimal lactic acid (ML) medium was that used to isolate Oscillospiraceae bacterium CPB6 (11). Full media recipes and protocols can be found in Supplementary Information (S.1.2.). Two stillage-based media were used to better mimic the bioreactor environment. Stillage media for glucose consumers (SG) consisted of solids-free thin stillage amended with 0.95 g $NH_4Cl \cdot L^{-1}$, pH corrected to 5.5 with 2 M NaOH, and 15 g $agar \cdot L^{-1}$. SG medium was autoclaved for 20 min at 121°C, after which the broth was used to pour plates. Stillage media for lactic acid consumers (SL) was identical, but 6.22 g Na-$lactate \cdot L^{-1}$ (i.e., 5 g $lactate \cdot L^{-1}$) was added before autoclaving.

A suspension of 0.5 mL of granular biofilm in 10 mL filter sterilized (0.20 µm) reactor effluent was first vortexed (3 x 30 seconds) until biofilm was fully disintegrated. This

suspension was then diluted 10^4 times in an anaerobic (10% CO_2, 90% N_2) chamber (GP-Campus, Jacomex, TCPS NV, Rotselaar, Belgium) to reach a cell concentration of approx. 10^5 cells·mL^{-1} based on flow cytometric cell counts (Accuri C6+, BD Biosciences). This cell suspension was serially diluted in down to 10 cells·mL^{-1}, and 100 µL of each serial dilution (10^4-10^1 cells·mL^{-1}) was spread onto each of the four media types. Plates had been in the anaerobic chamber for at least 1h to release all dissolved O_2 from the plate. Plates were incubated inside the anaerobic chamber at 37°C for 7 days (SG, SL, MG), or 14 days (ML). After incubation, fifteen colonies were arbitrarily picked from each type of medium. Picked colonies were spread onto fresh plates of their original medium and incubated for the same time, except isolates on ML medium, which were transferred to SL plates to increase biomass density per colony. Each isolate was designated with an identifier made up of the medium type (i.e., SG, SL, MG, or ML) and their number (1-15). Streak-purified colonies were picked and stored in microcentrifuge tubes (Micrewtube, VWR) at -20°C for later DNA extraction and full-length 16S rRNA gene sequencing for identification and FISH probe design.

2.3. ^{15}N-incubation of fermentative granular biofilms

Granules were incubated with $^{15}NH_4Cl$ in miniaturized EGSB bioreactors (V=60 mL) for later growth activity analysis with FISH-nanoSIMS (21,24). First, feed was prepared by amending solids-free thin stillage with 12% $^{15}NH_4Cl$ (0.836 g $NH_4Cl·L^{-1}$ and 0.116 g $^{15}NH_4Cl·L^{-1}$). Initial reactor broth was prepared by centrifuging effluent from the main EGSB reactor at 24 610 g for 15 minutes to remove suspended biomass, followed by amending with 0.116 g $^{15}NH_4Cl·L^{-1}$ to achieve an initial 12% $^{15}NH_4Cl$. To identify competitive-cooperative interactions in the community, growth activity in solid-free thin stillage was compared to that in lactate-supplemented (5 g lactate·L^{-1}) solid-free thin stillage. During incubation, pH was corrected manually to 5.5 with 2 M NaOH every 30 minutes. After 4 and 8 hours, 5 mL supernatant was sampled and filtered (0.20 µm) for soluble product analysis. Granular biomass was sampled

after 8 hours and washed by gently adding 8 mL phosphate buffered saline (PBS) at pH 5.5 to 2 mL of granular biomass, letting the granules settle (approx. 10s), and taking off supernatant containing suspended biomass. This was repeated at least 4 times, or until the supernatant was free of suspended biomass. After washing, granules were fixed by adding 9 mL of a PBS-solution at pH 5.5 containing 4% paraformaldehyde. After overnight fixation at 4°C, granules were washed 3 times in PBS at pH 5.5 and ultimately stored at 4°C in 10 mL of 1:1 PBS:ethanol.

2.4. FISH-nanoSIMS analysis

Tandem FISH-nanoSIMS analysis was used to visualize spatial organization and growth activity patterns in MCCA producing granular biofilms. Fixed granules were first embedded in agar (2% Noble agar in PBS), and then in Technovit 8100 following protocols described by McGlynn et al. (21). The block of resin was manually trimmed in half, after which 2 µm sections were obtained with a Leica glass-knife microtome. Sections were deposited on poly L-lysine-coated microscope slides coated with Teflon wells. FISH was conducted using standard protocols (25) on these sections, using 30% formamide during hybridization, and a hybridization time of 1.5h. Sections were then mounted in a mixture of DAPI and Citifluor (5 µg/mL), and covered with a coverslip. An epifluorescence mapping microscope (Elyra 7, Zeiss Microscopy) equipped with a Plan-APOCHROMAT 100x objective was used for microscopic imaging at Caltech. Images were captured by serial illumination of sections with 642 nm, 561 nm, 488 nm, and 405 nm lasers for 1 second and capturing fluorescent light. Frames (80 µm x 80µm) were captured sequentially and stitched together with Zen Black-software.

After FISH imaging, the coverslip was removed and slides were gently washed with deionized water, dried at room temperature. Slides were then cut into pieces to fit into the nanoSIMS holders, and sputter coated with a 30 nm gold layer before analysis on a CAMECA nanoSIMS 50L at the Center for Microanalysis at Caltech cf. McGlynn et al. (21). Samples

were first pre-sputtered with a high-intensity 90 pA Cs^+ ion beam until a stable signal (approx. 15,000 cps) was obtained on the $^{14}N^{12}C$-channel. Subsequently, a low-intensity Cs^+ ion beam (0.3 pA) was used to analyse 30x30 µm rasters, collecting data for $^{15}N^{12}C$, $^{14}N^{12}C$, and ^{12}C ions, where accumulation of ^{15}N in cells was determined by measurement of $^{15}N^{12}C$ and $^{14}N^{12}C$-ions. To assess activity gradients in the biofilm, transects were analyzed running either from the polar (i.e., the flat surface of the disc-shaped biofilm) or equatorial (i.e., the rim of the disc) periphery of the lenticular biofilms for at least 350 µm.

After data collection, nanoSIMS data were analysed in a pipeline modified from McGlynn et al. (21). Look@NanoSIMS (LANS) software (26) was used to pre-process data, while assignment of regions of interest (ROI) was performed manually with a custom MATLAB script (21). Three classes of ROI were identified based on FISH-microscopy: (i) Oscillospiraceae-cells, (ii) *Olsenella*-cells, and (iii) other bacteria. Spatial coordinates of cells were obtained in MATLAB by manually tracing an outline of the granular biofilm and calculating the pairwise distance between the biofilm surface and the center of each assigned cell.

2.5. Chemical analyses

C3 to C8 carboxylic acids (including isoforms C4 to C6) were determined by gas chromatography (27). Lactic and acetic acid concentrations were determined by ion chromatography (28). Full analytical methods can be found in Supplementary Information (S.1.3.)

2.6. Molecular methods

DNA was extracted from picked colonies by phenol-chloroform extraction as described before (29), except using a MoBio Powerlyzer 24 during the bead beating step for 2 cycles of 5 minutes at 2,000 rpm. The 16S rRNA gene was PCR-amplified with 63F (30) and 1378R (31) primers, followed by purification with the innuPREP PCR cleanup kit (Westburg, The

Netherlands) and Sanger sequenced at LGC genomics (Middlesex, UK). Sequences were identified by the NCBI Basic Local Alignment Search Tool (BLAST, https://blast.ncbi.nlm.nih.gov/), and isolates belonging to *Olsenella* and Oscillospiraceae – cf. earlier reports (5) - were retained. These new sequences and a set of closest relatives were aligned in MEGA X (32) using the Multiple Sequence Comparison by Log-Expectation (MUSCLE) alignment tool. A phylogenetic tree was constructed with the Maximum Likelihood algorithm, using the Tamura-Nei model (33) to calculate phylogenetic distances, and performing bootstrap analysis (n=500) to assess the reliability of each branch. To validate the representativeness of the isolates, the 16S rRNA gene amplicon sequencing dataset reported in Carvajal-Arroyo et al. (5) was reclassified with the new full-length 16S rRNA gene sequences obtained from the isolation campaign. Using TaxAss (34), the V3-V4 sequences were classified against a custom database containing three isolates (1 *Olsenella*, 2 Oscillospiraceae). Sequences with a match of at least 98% to the new isolate sequences were classified as these isolates, while the remaining sequences were classified with the SILVA v138 database as reported previously (5).

FISH probes were designed to visualize the spatial organization of species in granular biofilms. Probes were developed with the PROBE_DESIGN tool from ARB-SILVA, using the full SILVA v128 database as reference (35,36). The design parameters of the probes were a length of 18-22 bp, a theoretical melting temperature of 40-65°C, and a GC-content of 50-60%. Two novel probes were designed: Ols-83 targeting *Olsenella* species isolated here, and Osc-140 targeting the two Oscillospiraceae isolates identified here, Oscillospiraceae bacterium CPB6 (11), and *Caproiciproducens galactitolivorans* (12) (Table 1).

232 **Table 1.** FISH probes used in this study

Probe name	Sequence (5'-3')	Target species	Dye	Reference
EUB-338-I	GCTGCCTCCCGTAGGAGT	All bacteria	Cy3	(37)
EUB-338-II	GCAGCCACCCGTAGGTGT	All bacteria	Cy3	(38)
EUB-338-III	GCTGCCACCCGTAGGTGT	All bacteria	Cy3	(38)
Ols-83	GCCACTTTATTCCCACCCGAA	Isolate SL2	Cy5	This study
Osc-140	CCAGACGTTATCCCCCTCTG	Isolates MG10 & MG12, Oscillospiraceae CPB6, *Caproiciproducens galactitolivorans*	6-FAM	This study

233

3. Results

3.1. Three novel isolates represent half of the MCCA producing granular biofilm community

An isolation campaign yielded 60 streak-purified isolates, of which 40 yielded full-length 16S rRNA gene sequences and another 7 yielded partial 16S rRNA gene sequences. 25 out of these 47 sequences were most closely related to Lactobacillaceae species (10 *Lentilactobacilli*, 9 *Lactiplantibacilli*, and 6 *Lacticaseibacilli*), 14 to *Olsenella* and 6 to *Caproiciproducens*, while the 2 remaining isolates were most closely related to *Clostridium* and *Neglecta* species (Figure 2A). Full-length 16S rRNA gene sequences of three isolates (SL2, MG10 and MG12) most closely related to dominant OTU identified in prior work (5) were used to reclassify amplicon sequencing data with TaxASS (34). The 3 selected isolates together represented approximately half of the granular biofilm community (54.8±9.9%, n=6), while in their respective genera, SL2 represented 84.8±6.6% of *Olsenella* members, and MG10 and MG12 together represented 51.4±10.2% of recovered *Caproiciproducens* OTUs. All three isolates were relatively distantly related to known organisms. Isolate SL2 likely represented a novel species within *Olsenella* based on 95.5-96.3% sequence identity to other *Olsenella* members and a distant branching point (Figure 2B). Isolate MG10 was most closely related to *Caproicibacterium amylolyticum* and Oscillospiraceae bacterium CPB6, both of which were isolated from fermentation pits for Chinese strong-flavour liquor (11,39). Based on the 97.9% 16S rRNA gene identity with *Caproicibacterium amylolyticum*, isolate MG10 may represent a new species within *Caproicibacterium*. Last, isolate MG12 was most closely related to *Caproiciproducens* organisms, although this genus is still under debate (40,41). Regardless, with less than 95% full length 16S rRNA gene identity, isolate MG12 hints at unidentified MCCA producing genera within Oscillospiraceae. Unfortunately, these isolates (SL2, MG10, MG12) could not be propagated on liquid or solid media, preventing characterization of these isolates' metabolism and physiology, and preventing deposition of these strains in culture collections.

Together, these isolates were considered representative of fermentative granular biofilms and were used for FISH probe design to analyze spatial organization in the biofilm.

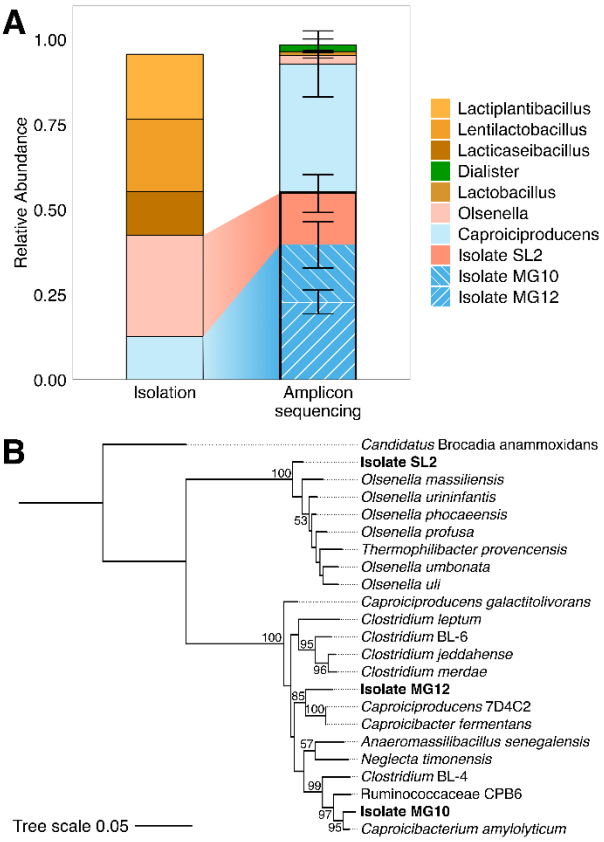

Figure 2. Representativeness of isolates from fermentative granular biofilms. Panel A shows (i) community composition from BLAST-identification of 47 partial or complete 16S rRNA gene sequences obtained through isolation, (ii) TaxASS reclassification of the dataset from Carvajal-Arroyo et al. (5) using a custom database of three isolates (SL2, MG10 and MG12) as well as the general SILVA v138 database. Only genera with a mean relative abundance higher than 1% are shown. Error bars indicate standard deviation over average community composition (n=6). Panel B shows the phylogenetic tree of the three representative isolates, along with closest relatives and relevant isolates from literature. Bootstrap values greater than or equal to 50% are shown as percentages at each node. Scale indicates substitutions per nucleotide position.

3.2. Spatial organization of granular biofilm communities

FISH-micrographs revealed *Olsenella* and Oscillospiraceae members co-occur and are well-mixed in the outer layers (150-500 µm) of the biofilm (Figure 3, Figure S.2.). Deeper in the biofilm, other community members become more dominant. Single cell identification with FISH along 4 transects (Figure 3C-I) confirm this observation (Figure 4A-D); near the biofilm

surface, Oscillospiraceae and *Olsenella* make up more than three quarters of all cells, while more than 250 µm into the biofilm they represent only 25-50% of the biofilm, with the remaining 50-75% of cells being other Bacteria (Figure 4A-D). These trends were observed across different transects within a single granular biofilm, and in both analyzed granules from either experimental condition (i.e., thin stillage, or thin stillage + lactic acid; Figure 4E). Together, these data show lactic acid producers and MCCA producers are not stratified within the biofilm but there is stratification of the catalytic community (*Olsenella*, Oscillospiraceae) at the outside, and the remaining microbial community towards the inside of the biofilm.

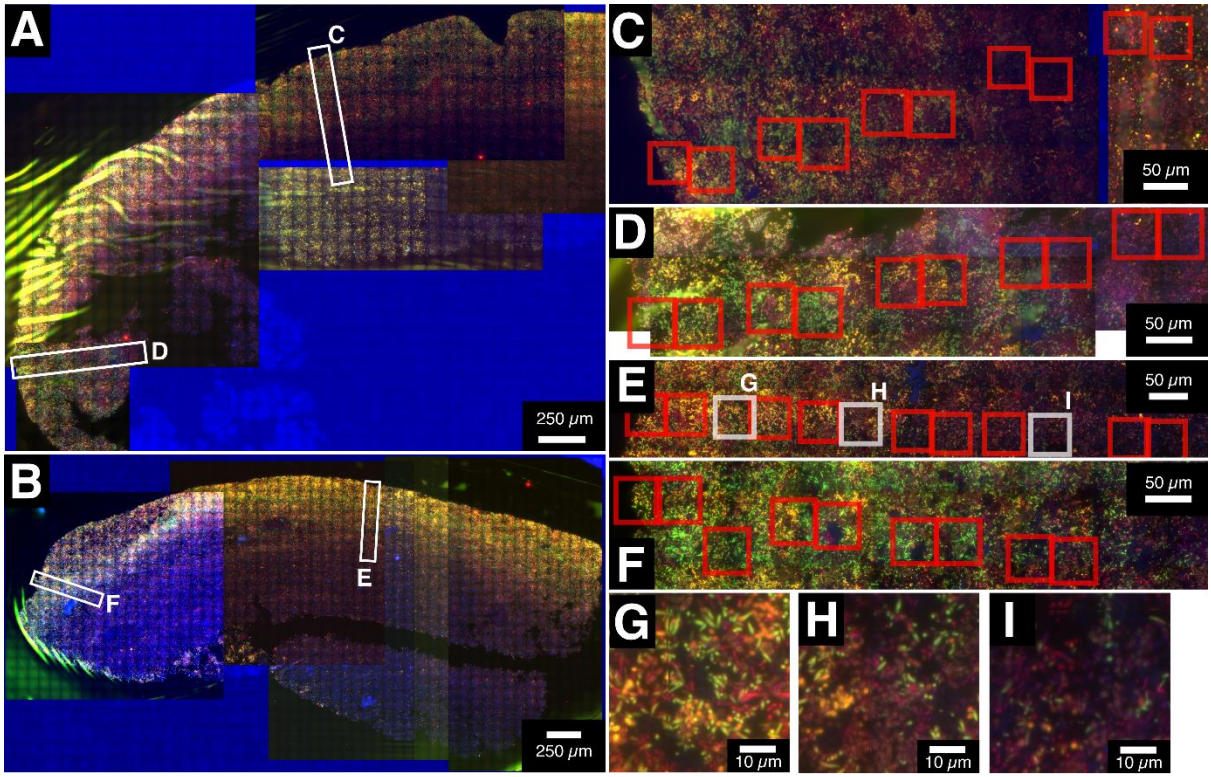

Figure 3. FISH micrographs of fermentative granular biofilms. Panel A and B show granular biofilms grown in respectively thin stillage and thin stillage amended with 5 g lactate·L^{-1}. Note that individual captures were linearly corrected for optimum signal display and then stitched together, creating technical artefacts in signal intensity between captures. White rectangles identify transects used for single-cell identification and activity analysis for polar (C, E) and equatorial (D, F) transects. In Panels C-F, red squares identify areas with single cell identification and activity analysis. Panels G-I show selected areas from transect E at full resolution. All images are false-colored composite images, displaying hybridization with Osc-140 (green), Ols-83 (yellow), and EUB-338-I,II,III (red) FISH probes, and DNA staining with DAPI (blue).

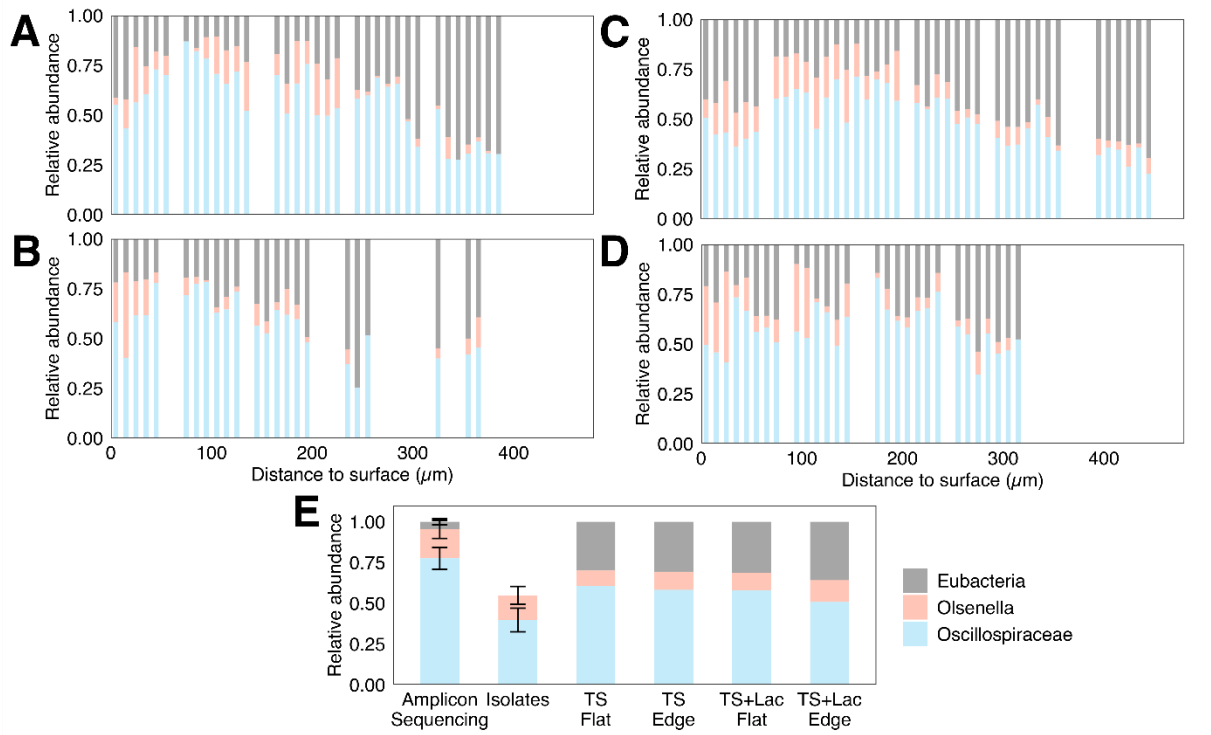

Figure 4. Spatial organization of key members of granular biofilms. Distribution of FISH-identified community members in granules grown in thin stillage (Panel A, polar transect, n=3,832; Panel B, equatorial transect, n=2,818) and in thin stillage amended with 5 g lactic acid·L^{-1} (Panel C, polar transect, n=4,104; Panel D, equatorial transect, n=2,805). Each bar represents at least 20 cells. Panel E compares community composition based on 16S rRNA gene amplicon sequencing from Carvajal-Arroyo et al. (5), TaxASS reclassification of those data based on isolate sequences, and the aggregate count-based community composition along each transect.

3.3. Anabolic activity is controlled by depth in the biofilm but not by transect location

Gradients of ^{15}N-incorporation were observed in all transects, with the highest growth activities observed near the surface, and average ^{15}N-content steadily decreased towards background levels around 300-400 µm in the biofilm (Figure 5). In solids-free thin stillage, anabolic activity at the polar edge was consistently higher than at the equatorial edge (Figure 5A). Comparing ^{15}N-assimilation levels between polar and equatorial edge in 100 µm bins confirmed that anabolic activity at the polar edge was significantly higher than at the equatorial edge in the first 200 µm (Figure S.3.). For instance, median ^{15}N incorporation in the outer 100 µm of the polar transect (4.83% ^{15}N) was significantly lower (p=9·10^{-5}, n=2,012) than that in the equatorial transect (4.58% ^{15}N), counter to the proposed hypothesis for lenticular biofilm

morphology. For transects in lactic acid-amended granular biofilms (Figure 5B), no significant difference in median anabolic activity was observed in the outer 100 μm (equatorial - 3.70% ^{15}N, polar – 3.67% ^{15}N, p=0.94, n=2,092). Transects deeper than 100 μm did show statistically significant differences of ^{15}N-content, but no cohesive pattern of higher anabolic activity was observed (Figure S.3.). Together, these data suggest that the lenticular morphology was not driven by anabolic activity gradients shaped by product inhibition, and substrate diffusion may be the primary process governing spatial patterns of anabolic activity. It is important to note that the activity gradient was not driven by diffusion limitation of $^{15}NH_4Cl$ into the biofilm, as cells with high activity (3.5-4.4% ^{15}N incorporated, with 12% ^{15}N supplied) could still be observed over 350 μm from the surface of the biofilm. While the general trend in activity may be driven by substrate diffusion gradients, these high-activity outliers deeper in the biofilm may have been associated with secondary activities such as biomass degradation and necrotrophic growth. Additionally, it is worth noting that these transects were compared in 2 granules (i.e., one granule per experimental condition). While the differences between transects within these granules are robust, this data does not account for cross-granule variability. Overall, the anabolic activity of single cells was governed by depth in the granular biofilm, which may be associated with diffusion limitations of carbon substrates into the biofilm.

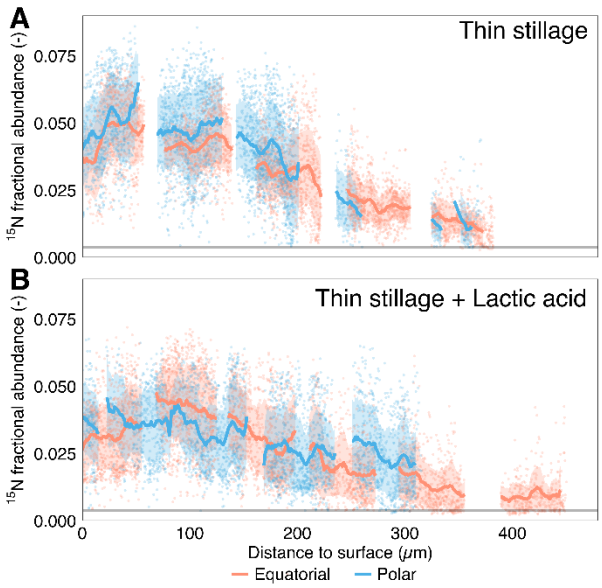

Figure 5. Single-cell anabolic activity across transects within disc-shaped biofilms. Panel A presents biofilms grown in regular conditions; Panel B shows biofilms grown supplemented with 5 g lactic acid·L^{-1}. Dots represent individual cells, lines and shaded areas represent moving window averages and standard deviations respectively over a 10 µm window. Grey band represents natural ^{15}N abundance range.

3.4. Lactic acid supplementation reduces anabolic activity of MCCA producers

Lactic acid supplementation stimulated lactic acid consumption and caproic acid production (Figure S.4.) but decreased the anabolic activity of some of the community members in the MCCA-producing granular biofilm (Figure 6). Lactic acid amendment decreased median ^{15}N content of Oscillospiraceae in the outer 100 µm of the polar transect by nearly 25% from 5.35% ^{15}N to 4.07% ^{15}N (p=1.9·10^{-48}, n=1137), while a decrease of approx. 15% was observed in the outer 100 µm of the equatorial transect, from median values of 4.94% ^{15}N to 4.19% ^{15}N (p=4.4·10^{-24}, n=1270). *Olsenella*-cells in the outer 100 µm of the biofilm were much less affected by lactic acid amendment. In the polar transect, no significant change was observed under lactic acid amendment (p=0.75, n=287), while *Olsenella* cells in the equatorial transect had a minor, but significant (p=0.024, n=369), decrease in ^{15}N-content, from median values of 4.23 %^{15}N (thin stillage) to 4.18% ^{15}N (thin stillage + lactic acid). Lactic acid amendment also decreased median ^{15}N content for cells in the outer 100 µm stained only with the Eubacterial

FISH probe. In both the polar transect – from 3.41% ^{15}N to 2.36% ^{15}N (p=3.0·10^{-11}, n=415) – and the equatorial transect – from 3.28% ^{15}N to 2.20% ^{15}N (p=4.2·10^{-16}, n=626) – the anabolic activity of other bacterial cells (i.e., hybridized with neither the *Olsenella* nor Oscillospiraceae-targeting FISH probes) decreased by more than 30%. This decreased activity could either be a direct response of the satellite community to lactic acid amendment or could be the result of decreased activity of Oscillospiraceae-members not covered by the Osc-140 FISH probe, although it is not possible to differentiate between these mechanisms based on the available data. These observations were also robust when pooling both equatorial and polar transects together (Figure S.5.) Together, these data suggest that lactic acid-supplementation increased MCCA-production but decreased the anabolic activity of MCCA producing Oscillospiraceae by 15-25%, while lactic acid-producing *Olsenella* maintained a similar level of activity across the granular biofilm analyzed from either incubation.

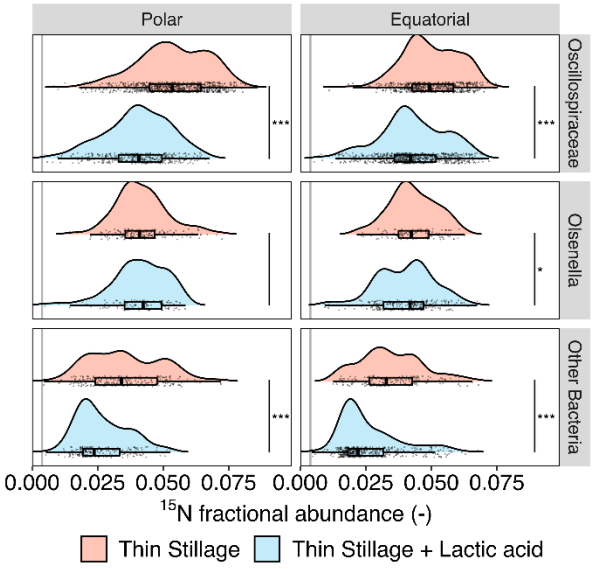

Figure 6. Anabolic activity response to lactic acid amendment per taxonomic group and per transect. Single cell anabolic activity – measured as ^{15}N incorporation – in the outer 100 µm of the granular biofilm are shown with dot plots representing individual cells, box plots, and distribution estimates. Activities in granules grown on thin stillage (red) were compared to granules grown on thin stillage amended with 5 g lactic acid·L^{-1} (blue). All data come from transects in a single biofilm from either condition. Sample groups were compared with Wilcoxon rank sum test: *, p<0.05; **, p<0.01; ***, p<0.001. Grey bands indicate natural abundance range of ^{15}N.

4. Discussion

4.1. Growth activity patterns do not drive lenticular biofilm morphology

We hypothesized that the lenticular biofilm morphology was the result of diffusion gradients of toxic MCCA favoring growth along a plane to minimize diffusion pathlengths (Figure 1). Growth activities at the polar edge were similar, or higher, than at the equatorial edge (Figure 3, 5, S.3.), implying that the lenticular morphology was not due to spatial patterns of growth activity influenced by caproic acid diffusion gradients. We cannot rule out the possibility that growth rates were saturated at both polar and equatorial peripheries, and instead, cells at the equatorial periphery transformed more carbon into extracellular polymeric substances (EPS), contributing to biofilm construction without nitrogen assimilation (42). Additionally, the short incubation time (8 hours) and initial disturbance may have temporarily altered activities and *in-situ* chemical gradients, however, this effect is expected to have been minor given the high observed growth activities and representative MCCA production rates of 6 g caproic acid·L^{-1}·h^{-1} (Figure S.4). Alternatively, breakage of large granular biofilms may alter morphology by creating smaller, and less spherical granules, which in turn can start growing again (43). The granular biofilms observed here display signs of breakage, i.e., the broken periphery lacks cells with high FISH signals (as proxy for activity) and displays a torn appearance (Figure 3A,B, Figure S.2). The difference in growth rate between the broken and intact biofilm peripheries could drive growth along a plane, eventually shaping the lenticular morphology during continuous granule breakage under hydraulically fluidized conditions (Figure 7). This alternative hypothesis also aligns with the observation that high organic loading rates induce lenticular morphologies (5), as higher growth rates could magnify the difference in growth rates at the active and broken biofilm peripheries. The observation of regular biofilm morphologies and size distributions (5) may in turn be due to shear and hydraulic factors. Crucially, the structural and physical properties of these granular biofilms and their response

to organic loading rates are currently uncharacterized. Additionally, while the described morphology was observed across multiple granules (Figure 3, Figure S.2.), expanding this analysis to a broad set of granules could further elucidate mechanisms of lenticular biofilm development. Further research is critical to elucidate the role of chemical gradients and physical processes that may shape the lenticular morphology of MCCA producing granular biofilms.

4.2. Lactic acid and MCCA producers compete for carbohydrates in the biofilm periphery

Granular biofilms producing MCCA were hypothesized to be stratified into a layer with lactic acid producing *Olsenella* at the periphery, and a lactic acid consuming MCCA producing Oscillospiraceae deeper in the biofilm (Figure 1). Following this rationale, amendment of lactic acid was expected to alleviate substrate limitation, increasing both MCCA production rates and ^{15}N incorporation. Contrary to this hypothesis, FISH images showed that *Olsenella* and Oscillospiraceae cells were well mixed in the outer layers of the biofilm (Figure 3, 4, Figure S.2). Further, lactic acid amendment increased MCCA production rates (Figure S.4.) but decreased anabolic activity of Oscillospiraceae (Figure 6), indicating that Oscillospiraceae-biomass yield per unit MCCA produced dropped.

It is worth noting that analyzing anabolic activities in a single granule for each condition may limit the conclusions drawn from these data, as it does not address potential variability between individual granular biofilms. However, the selected granules may be representative of the average community. First, trends in anabolic activity were observed in 2 transects within a biofilm, despite being approx. 1 mm apart (Figure 3, Figure S.5.). Second, the communities in these granules were ecologically stable, with little variability over 200 days of operation (5), and remaining stable for years across different studies, including this report (7,8, Figure 2). Last, community composition across individual granules in an aerobic granular biofilm system

were shown to be cohesive at the genus-level (44), suggesting functionality may also be similar across individual biofilms. Together, this suggests that variability across granules may be limited, although the data presented here cannot fully quantify inter-granule variation.

Assuming cross-granule variability is limited, three phenomena could explain the simultaneous decrease in ^{15}N-activity and increase in product formation: (i) MCCA production was taken over by another taxonomic group, (ii) MCCA toxicity increased energy requirements for cell maintenance, or (iii) lactic acid amendment induced a shift from sugars to lactic acid as substrate for MCCA producing Oscillospiraceae. The first hypothesis is unlikely, as ^{15}N-incorporation did not increase for other bacterial groups (Figure 5), although we cannot fully rule out that a small subpopulation increased in activity. In the second case, MCCA toxicity disrupting cell processes would increase maintenance energy requirements, reducing cell yield per mol of MCCA produced. For instance, previous research has shown that lower pH increased MCCA toxicity and halved biomass yield on ethanol as a substrate (45). Here, an increase of caproic acid from 2.1 to 2.7 g·L^{-1} (18.1 to 23.2 mM) at the end of the 8-hour incubations (Figure S.4.) resulted in a 15-25% decrease in ^{15}N-incorporation (Figure 6). Extrapolating these data based on the negative linear relationship between growth rate and MCCA concentration (16,17) yields toxicity limits of 4.5-6.1 g·L^{-1}. Given that a previous report obtained up to 6.8 g caproic acid g·L^{-1} (5), toxicity alone may not fully explain the decreased cell yield. Last, Oscillospiraceae switching its carbon/electron source from sugar to lactic acid would release less than a third of the Gibbs Free energy yield (Supplementary Information, S.2.5.) per MCCA produced, lowering ATP-yield, cell growth and ^{15}N-incorporation. For instance, in *Megasphaera hexanoica*, this shift was shown to reduce biomass yield per mol MCCA produced by 80% (13). Since lactic acid was always in excess during lactic acid amended incubations (Figure S.4.), this may have been the more attractive substrate, driving the observed reduction in ^{15}N-incorporation per MCCA produced. Unfortunately, this

hypothesis could not be tested, as isolates obtained by plating (Figure 2) could not be propagated on liquid, nor on solid media. The shift from sugars to lactic acid as substrate suggests that Oscillospiraceae may be competing for sugars with lactic acid producers under normal operation (Figure 7). While there is no direct evidence of niche overlap, a scenario in which *Olsenella* and Oscillospiraceae consume different carbohydrate pools in the feedstock cannot support the observed simultaneous increase in MCCA-production and decrease in ^{15}N incorporation by Oscillospiraceae. Additionally, substrate competition between lactic acid and MCCA producers has been suggested previously based on the functionality of closely related isolates (46), metagenome-identified functions (47), and flux-balance analysis (48), but this report presents the first *in situ* observation of this interaction.

Substrate competition between *Olsenella* and Oscillospiraceae may also provide context for their spatial co-occurrence in the biofilm within the top 200-300 µm deep catalytic layer, as observed by FISH (Figure 3, Figure 7). Carbohydrates could be consumed by both *Olsenella* and Oscillospiraceae in the catalytic layer, while an inner core enriched in other community members may drive secondary conversions, such as the breakdown of dead microbial biomass and EPS making up the biofilm matrix (Figure 3, 4). In other granular biofilm systems, chemical gradients of e.g., O_2 or carbon substrates stratify core functional guilds involved in e.g., nutrient removal, or methane production (18–20). Since the two major functional guilds – lactic acid producing *Olsenella* and MCCA producing Oscillospiraceae – in this system appear to compete for carbohydrates, they can coexist near the biofilm periphery. The continued coexistence of *Olsenella* and Oscillospiraceae in these biofilms does imply some niche differentiation must exist. Future research should investigate whether *Olsenella* have a kinetic (e.g., substrate affinities, growth rates) or substrate (e.g., a broader carbohydrate degrading repertoire) niche enabling their presence alongside carbohydrate consuming Oscillospiraceae. Moreover, the coexistence of Oscillospiraceae alongside *Olsenella* also suggests

Oscillospiraceae may consume sugars and lactic acid concomitantly. Further research should elucidate whether a single cell consumes both substrates simultaneously, or, whether sugar and lactic acid consuming Oscillospiraceae cells are spatially segregated in the biofilm.

Overall, MCCA producing granular biofilms are stratified in a catalytic layer where lactic acid and MCCA producers compete for carbohydrates, and an inner core potentially involved in biomass and EPS-degradation.

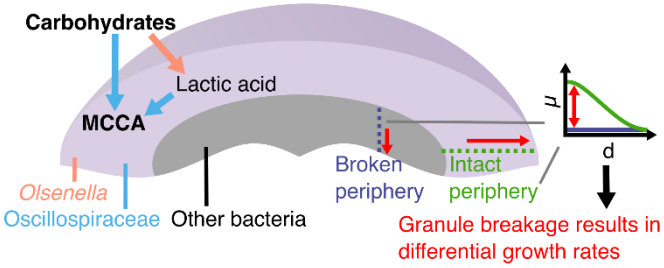

Figure 7. Revised, observation-based hypothesis of carbon fluxes and mechanisms of lenticular biofilm morphology

4.3. Implications for bioprocess development

The hypotheses describing MCCA producing granular biofilms presented here (Figure 7) also have implications for the development and optimization of MCCA bioproduction processes leveraging granular biofilms. If Oscillospiraceae convert carbohydrates directly to MCCA, *Olsenella* may not be a necessary functional guild in the community. Establishing an Oscillospiraceae-only community may prove beneficial if this improves product selectivity and/or process stability. However, if *Olsenella* have a broader substrate degradation range, or more favorable kinetic parameters, their ecological niche may improve process performance and may directly impact process optimization strategies. Alternatively, *Olsenella* could also play a role in biofilm development, e.g., EPS production. For instance, a recent report established lactic acid fed MCCA producing granular biofilms with a non-lenticular morphology but continued to observe *Olsenella* in the community (8). While abundances of

Olsenella in those lactic acid-fed biofilms were lower than what was observed in this study, they may still have contributed to biofilm formation, although this remains speculative given our current knowledge. Overall, understanding the roles of *Olsenella* besides lactic acid production may be critical to optimize the community for reliable, sustainable bioproduction of MCCA from complex feedstocks. Additionally, the role of the inner non-catalytic biofilm core in biofilm stability and catalytic efficiency may be significant at larger process scales. In a granule 4 mm wide, 1 mm high and with a 200 μm wide active periphery, only 51.4% of the granular biofilm volume is catalytically active. If only the outer rim is actively producing MCCA, controlling biofilm size could help maximize the catalytic volume (49,50). While the lenticular morphology increases catalytic efficiency compared to spherical biofilms (51), optimizing granule size may further benefit process performance. Granule sizes could be controlled using selective sludge separation or using shear as a controlling factor (52–54), while optimal sizes could be determined by identifying the minimal size at which effective catalytic volumes are maximized while granules still effectively settle and remain in the system. Such observations demonstrate the power of microbial ecological studies of granular biofilm systems to drive the development and optimization of bioprocesses. It will be critical to understand if higher catalytic volumes come at the cost of granular biofilm stability and density, which in turn would deteriorate process efficiency. Ultimately, identifying the ecological mechanisms underpinning this community will be critical to further develop and optimize granular biofilm technologies for MCCA production.

5. Conclusions

Granular biofilm technologies are a powerful approach to intensify bioprocesses but require understanding the underlying microbial interactions to inform process optimization and process control strategies. In this study, we investigated the spatial organization and microbial ecology of MCCA producing granular biofilms to understand their unique lenticular morphology. Counter to the proposed hypothesis, growth activity was not affected by the location within the biofilm (i.e., near the polar or equatorial periphery of the biofilm) which had been previously hypothesized to be highest at the equator of the biofilm. Second, the biofilm was observed to consist of an outer catalytic layer (150-500 μm) containing spatially well-mixed communities of lactic acid producing *Olsenella* and MCCA producing Oscillospiraceae, while inner layers were dominated by other bacteria potentially involved in biomass and EPS degradation. This observation directly points at opportunities for process optimization by controlling biofilm size. Third, Oscillospiraceae appear to switch from carbohydrates to lactic acid as substrate during lactic acid amendment. This suggests that MCCA producers may compete for carbohydrates with lactic acid producers under normal conditions, enabling their spatial co-occurrence in the biofilm. This competitive interaction had been hypothesized previously, but the single-cell anabolic activity data reported here may present the first *in situ* observation of this competitive interaction. This study provides novel insights into the spatial ecophysiology of MCCA producing granular biofilms that can guide the optimization (e.g., granular biofilm size, feed composition) and implementation of granular biofilm technologies for sustainable bioproduction.

6. Acknowledgements

P.C. was supported by UGent Special Research Fund (BOF15/DOC/286) and the U.S. Department of Energy, Office of Science, Office of Biological & Environmental Research (#DE-SC0020356). RG is supported by the Special Research Fund of Ghent University (grant number BOF19/STA/044). G.L.C. and V.J.O. were supported by grants from the Department of Energy, Office of Science, Office of Biological and Environmental Research (#DE-SC0020373). V.J.O. was also supported by the Simons Foundation PriME collaboration

7. Competing interests

The authors declare no financial or non-financial competing interests.

8. Data availability statement

16S rRNA gene sequences have been deposited to NCBI GenBank under accession numbers OP799682-OP799726

9. Author Contributions

Conceptualization: P.C., G.L.C., and J.M.C.A. Methodology: P.C., G.L.C. Investigation: P.C., G.L.C., T.L. Formal Analysis: P.C., G.L.C. Supervision: V.J.O., K.R. Writing – Original Draft: P.C. Writing – Review & Editing: All authors.

10. References

1. Agler MT, Spirito CM, Usack JG, Werner JJ, Angenent LT. Chain elongation with reactor microbiomes: upgrading dilute ethanol to medium-chain carboxylates. Energy Environ Sci. 2012;5(8):8189–92.
2. Angenent LT, Richter H, Buckel W, Spirito CM, Steinbusch KJJ, Plugge CM, et al. Chain Elongation with Reactor Microbiomes : Open-Culture Biotechnology To Produce Biochemicals. Environ Sci Technol. 2016;50(6):2796–810.
3. Urban C, Xu J, Sträuber H, dos Santos Dantas TR, Mühlenberg J, Härtig C, et al. Production of drop-in fuels from biomass at high selectivity by combined microbial and electrochemical conversion. Energy Environ Sci. 2017;10(10):2231–44.
4. Roghair M, Strik DPBTB, Steinbusch KJJ, Weusthuis RA, Bruins ME, Buisman CJN. Granular sludge formation and characterization in a chain elongation process. Process Biochemistry. 2016;51(10):1594–8.
5. Carvajal-Arroyo JM, Candry P, Andersen SJ, Props R, Seviour T, Ganigué R, et al. Granular fermentation enables high rate caproic acid production from solid-free thin stillage. Green Chemistry. 2019;21(6):1330–9.
6. Wu Q, Feng X, Chen Y, Liu M, Bao X. Continuous medium chain carboxylic acids production from excess sludge by granular chain-elongation process. J Hazard Mater. 2021 Jan 15;402:123471.
7. Mariën Q, Candry P, Hendriks E, Carvajal-Arroyo JM, Ganigué R. Substrate loading and nutrient composition steer caproic acid production and biofilm aggregation in high-rate granular reactors. J Environ Chem Eng. 2022;10(107727).
8. Mariën Q, Ulčar B, Verleyen J, Vanthuyne B, Ganigué R. High-rate conversion of lactic acid-rich streams to caproic acid in a fermentative granular system. Bioresour Technol. 2022;355(127250):1–10.

9. Smith AL, Stadler LB, Cao L, Love NG, Raskin L, Skerlos SJ. Navigating wastewater energy recovery strategies: A life cycle comparison of anaerobic membrane bioreactor and conventional treatment systems with anaerobic digestion. Environ Sci Technol. 2014;48(10):5972–81.

10. Dewhirst FE, Paster BJ, Tzellas N, Coleman B, Downes J, Spratt DA, et al. Characterization of novel human oral isolates and cloned 16S rDNA sequences that fall in the family Coriobacteriaceae : description of Olsenella gen . nov ., reclassification of Lactobacillus uli as Olsenella uli comb . nov . and description of Olsenella . Int J Syst Evol Microbiol. 2001;51:1797–804.

11. Zhu X, Zhou Y, Wang Y, Wu T, Li X, Li D, et al. Production of high-concentration n-caproic acid from lactate through fermentation using a newly isolated Ruminococcaceae bacterium CPB6. Biotechnol Biofuels. 2017;10(1):1–12.

12. Kim BC, Jeon BS, Kim S, Kim H, Um Y, Sang BI. Caproiciproducens galactitolivorans gen. Nov., sp. nov., a bacterium capable of producing caproic acid from galactitol, isolated from a wastewater treatment plant. Int J Syst Evol Microbiol. 2015;65(12):4902–8.

13. Kang S, Kim H, Jeon BS, Choi O, Sang BI. Chain elongation process for caproate production using lactate as electron donor in Megasphaera hexanoica. Bioresour Technol. 2022;346(126660):1–6.

14. Wang H, Li X, Wang Y, Tao Y, Lu S, Zhu X, et al. Improvement of n-caproic acid production with Ruminococcaceae bacterium CPB6: Selection of electron acceptors and carbon sources and optimization of the culture medium. Microb Cell Fact. 2018;17(1):1–9.

15. Candry P, Ganigué R. Chain elongators, friends, and foes. Curr Opin Biotechnol. 2021;67:99–110.

16. Royce LA, Liu P, Stebbins MJ, Hanson BC, Jarboe LR. The damaging effects of short chain fatty acids on Escherichia coli membranes. Appl Microbiol Biotechnol. 2013;97:8317–27.
17. Candry P, van Daele T, Denis K, Amerlinck Y, Andersen SJ, Ganigué R, et al. A novel high-throughput method for kinetic characterisation of anaerobic bioproduction strains, applied to Clostridium kluyveri. Sci Rep. 2018 Jun 27;8(9724):1–13.
18. Winkler MKH, Kleerebezem R, Van Loosdrecht MCM. Integration of anammox into the aerobic granular sludge process for main stream wastewater treatment at ambient temperatures. Water Res. 2012;46(1):136–44.
19. Winkler MKH, Kleerebezem R, Strous M, Chandran K, Van Loosdrecht MCM. Factors influencing the density of aerobic granular sludge. Appl Microbiol Biotechnol. 2013;97(16):7459–68.
20. Zheng D, Angenent LT, Raskin L. Monitoring granule formation in anaerobic upflow bioreactors using oligonucleotide hybridization probes. Biotechnol Bioeng. 2006;94(3):458–72.
21. Mcglynn SE, Chadwick GL, Kempes CP, Orphan VJ. Single cell activity reveals direct electron transfer in methanotrophic consortia. Nature. 2015;526:531–5.
22. Dawson KS, Scheller S, Dillon JG, Orphan VJ. Stable isotope phenotyping via cluster analysis of NanoSIMS data as a method for characterizing distinct microbial ecophysiologies and sulfur-cycling in the environment. Front Microbiol. 2016;7(774):1–15.
23. Jeon BS, Kim BC, Um Y, Sang BI. Production of hexanoic acid from d-galactitol by a newly isolated Clostridium sp. BS-1. Appl Microbiol Biotechnol. 2010;88(5):1161–7.
24. Kopf SH, McGlynn SE, Green-Saxena A, Guan Y, Newman DK, Orphan VJ. Heavy water and 15N labelling with NanoSIMS analysis reveals growth rate-dependent

metabolic heterogeneity in chemostats. Environ Microbiol. 2015;17(7):2542–56.

25. Fuchs BM, Pernthaler J, Amann R. Single cell identification by fluorescencein situ hybridization. In: Reddy CA, Beveridgje TJ, Breznak JA, Marzluf GA, Schmidt TM, Snyder LR, editors. Methods for general and molecular microbiology. 3rd Edition. Washington D.C.: ASM Press; 2007. p. 886–96.

26. Polerecky L, Adam B, Milucka J, Musat N, Vagner T, Kuypers MMM. Look@NanoSIMS – a tool for the analysis of nanoSIMS data in environmental microbiology. Environ Microbiol. 2012;14(4):1009–23.

27. Andersen SJ, Candry P, Basadre T, Khor WC, Roume H, Hernandez-Sanabria E, et al. Electrolytic extraction drives volatile fatty acid chain elongation through lactic acid and replaces chemical pH control in thin stillage fermentation. Biotechnol Biofuels. 2015;8(221):1–14.

28. Gildemyn S, Verbeeck K, Slabbinck R, Andersen SJ, Prévoteau A, Rabaey K. Integrated production, extraction, and concentration of acetic acid from CO2 through microbial electrosynthesis. Environ Sci Technol Lett. 2015;2(11):325–8.

29. Geirnaert A, Wang J, Tinck M, Steyaert A, Van den Abbeele P, Eeckhaut V, et al. Interindividual differences in response to treatment with butyrate-producing Butyricicoccus pullicaecorum 25-3T studied in an in vitro gut model. FEMS Microbiol Ecol. 2015;91(6):1–12.

30. Marchesi JR, Sato T, Weightman AJ, Martin TA, Fry JC, Hiom SJ, et al. Design and evaluation of useful bacterium-specific PCR primers that amplify genes coding for bacterial 16S rRNA. Appl Environ Microbiol. 1998;64(2):795–9.

31. Heuer H, Krsek M, Baker P, Smalla K, Wellington EMH. Analysis of actinomycete communities by specific amplification of genes encoding 16S rDNA and gel-electrophoretic separation in denaturing gradients. Appl Environ Microbiol.

1997;63(8):3233–41.

32. Kumar S, Stecher G, Li M, Knyaz C, Tamura K. MEGA X: Molecular evolutionary genetics analysis across computing platforms. Mol Biol Evol. 2018;35(6):1547–9.

33. Tamura K, Nei M. Estimation of the Number of Nucleotide Substitutions in the Control Region of Mitochondrial DNA in Humans and. Mol Biol Evol. 1993;10(3):512–26.

34. Rohwer RR, Hamilton JJ, Newton RJ, McMahon KD. TaxAss: Leveraging a Custom Freshwater Database Achieves Fine-Scale Taxonomic Resolution. mSphere. 2018;3(5):1–14.

35. Ludwig W, Strunk O, Westram R, Richter L, Meier H, Yadhukumar A, et al. ARB: a software environment for sequence data. Nucleic Acids Res. 2004;32(4):1363–71.

36. Quast C, Pruesse E, Yilmaz P, Gerken J, Schweer T, Yarza P, et al. The SILVA ribosomal RNA gene database project: improved data processing and web-based tools. Nucleic Acids Res. 2013 Jan 1;41(D1):D590–6.

37. Amann RI, Binder BJ, Olson RJ, Chisholm SW, Deverux R, Stahl DA. Combination of 16S rRNA-targeted oligonucleotide probes with flow cytometry for analyzing mixed microbial populations. Appl Environ Microbiol. 1990;56(6):1919–25.

38. Daims H, Bruhl A, Amann R, Schleifer K heinz, Wagner M. The Domain-specific Probe EUB338 is Insufficient for the Detection of all Bacteria : Development and Evaluation of a more Comprehensive Probe Set. Syst Appl Microbiol. 1999;22:434–44.

39. Gu Y, Zhu X, Lin F, Shen C, Li Y, Ao L, et al. Caproicibacterium amylolyticum gen. Nov., sp. nov., a novel member of the family oscillospiraceae isolated from pit clay used for making chinese strong aroma-type liquor. Int J Syst Evol Microbiol. 2021 Apr 27;71(4):004789.

40. Esquivel-Elizondo S, Bağcı C, Temovska M, Jeon BS, Bessarab I, Williams RBH, et al. The Isolate Caproiciproducens sp. 7D4C2 Produces n-Caproate at Mildly Acidic

Conditions From Hexoses: Genome and rBOX Comparison With Related Strains and Chain-Elongating Bacteria. Front Microbiol. 2021;11(3335):1–18.

41. Flaiz M, Baur T, Brahner S, Poehlein A, Daniel R, Bengelsdorf FR. Caproicibacter fermentans gen. Nov., sp. nov., a new caproate-producing bacterium and emended description of the genus caproiciproducens. Int J Syst Evol Microbiol. 2020;70(7):4269–79.

42. Staats N, Stal LJ, Mur LR. Exopolysaccharide production by the epipelic diatom Cylindrotheca closterium: effects of nutrient conditions. J Exp Mar Biol Ecol. 2000 Jun 1;249(1):13–27.

43. Trego AC, Galvin E, Sweeney C, Dunning S, Murphy C, Mills S, et al. Growth and Break-Up of Methanogenic Granules Suggests Mechanisms for Biofilm and Community Development. Front Microbiol. 2020;11(1126):1–12.

44. Leventhal GE, Boix C, Kuechler U, Enke TN, Sliwerska E, Holliger C, et al. Strain-level diversity drives alternative community types in millimetre-scale granular biofilms. Nature Microbiology 2018 3:11. 2018;3(11):1295–303.

45. Allaart MT, Stouten GR, Sousa DZ, Kleerebezem R. Product Inhibition and pH Affect Stoichiometry and Kinetics of Chain Elongating Microbial Communities in Sequencing Batch Bioreactors. Front Bioeng Biotechnol. 2021;9(513):1–9.

46. Andersen SJ, Groof V De, Khor WC, Roume H, Props R, Coma M, et al. A Clostridium Group IV Species Dominates and Suppresses a Mixed Culture Fermentation by Tolerance to Medium Chain Fatty Acids Products. Front Bioeng Biotechnol. 2017;5(8):1–10.

47. Scarborough MJ, Lawson CE, Hamilton JJ, Donohue TJ, Noguera DR. Metatranscriptomic and Thermodynamic Insights into Medium-Chain Fatty Acid Production Using an Anaerobic Microbiome. mSystems. 2018;3(6):1–21.

48. Scarborough MJ, Hamilton JJ, Erb EA, Donohue TJ, Noguera DR. Diagnosing and Predicting Mixed-Culture Fermentations with Unicellular and Guild-Based Metabolic Models. mSystems. 2020;5(5):1–19.
49. Nguyen Quoc B, Armenta M, Carter JA, Bucher R, Sukapanpotharam P, Bryson SJ, et al. An investigation into the optimal granular sludge size for simultaneous nitrogen and phosphate removal. Water Res. 2021;198(117119):1–12.
50. Nguyen Quoc B, Wei S, Armenta M, Bucher R, Sukapanpotharam P, Stahl DA, et al. Aerobic granular sludge: Impact of size distribution on nitrification capacity. Water Res. 2021 Jan 1;188:116445.
51. Krasňan V, Stloukal R, Rosenberg M, Rebroš M. Immobilization of cells and enzymes to LentiKats®. Appl Microbiol Biotechnol. 2016;100(6):2535–53.
52. Winkler MKH, Bassin JP, Kleerebezem R, de Bruin LMM, van den Brand TPH, van Loosdrecht MCM. Selective sludge removal in a segregated aerobic granular biomass system as a strategy to control PAO–GAO competition at high temperatures. Water Res. 2011 May 1;45(11):3291–9.
53. Winkler MKH, Kleerebezem R, Kuenen JG, Yang J, van Loosdrecht MCM. Segregation of biomass in cyclic anaerobic/aerobic granular sludge allows the enrichment of anaerobic ammonium oxidizing bacteria at low temperatures. Environ Sci Technol. 2011 Sep 1;45(17):7330–7.
54. Tay JH, Liu QS, Liu Y. The effect of upflow air velocity on the structure of aerobic granules cultivated in a sequencing batch reactor. Water Science and Technology. 2004;49(11–12):35–40.